GENOTYPING A THALASSEMIA POINT MUTATION BY PROBE-GATED SILICA NANOPARTICLES

by
Meltem Ercan

Submitted to Graduate School of Natural and Applied Sciences
in Partial Fulfillment of the Requirements
for the Degree of Master of Science in
Biotechnology

Yeditepe University
2017

GENOTYPING A THALASSEMIA POINT MUTATION BY PROBE-GATED SILICA NANOPARTICLES

APPROVED BY:

Assist. Prof. Dr. Bilge Güvenç Tuna ……
(Thesis Supervisor)

Assoc. Prof. Dr. Soner Doğan ……

Assist. Prof. Dr. Barış Ata Borsa ……

DATE OF APPROVAL: …./…./2017

ACKNOWLEDGEMENTS

First of all, I would like to thank to my supervisor, Assist. Prof. Dr. Bilge Güvenç Tuna and my co-supervisor Assoc. Prof. Dr. V. Cengiz Özalp for giving me encouragement, guidance and support with great patience during my study. Working in their guidance in this project was very honourable and valuable.

I would like to thank to Assoc. Prof. Dr. Dilek Telci for her support and help. I would also like to thank to Assist. Prof. Dr. Yasemin Yücel for her help and support.

I would like to thank Research Assistant Samet Uçak for his help and support. I am very glad to work together. I would also like to thank my friends Tutku Aksoy, Fulya Küçükcankurt, Zeynep Güngördü Dalar, and Hazel Erkan for their valuable advice, understanding and assistance during my thesis.

Finally, my deepest gratitude goes to my family for their endless love, unconditional support and faith. It is very special for me to dedicate my thesis to my lovely family.

ABSTRACT

GENOTYPING A THALASSEMIA POINT MUTATION BY PROBE-GATED SILICA NANOPARTICLES

β-thalassemia is an inherited blood disorder that can lead to anemia. The causative reason for the disease is known to be mutation(s) in hemoglobin (HBB) gene that produces one of the subunits, called beta hemoglobin. Mutations in the HBB gene can reduce or abolish the production of beta-hemoglobin leading to abnormal hemoglobin protein structure and thus reduced oxygen carrying capacity. Therefore, low number of red blood cells in the blood causes the person's ability to produce hemoglobin and associated anemia complications.

The development of simple, reliable, and rapid approaches for molecular detection of common mutations is important for prevention and early diagnosis of genetic diseases, including Thalassemia. Oligonucleotide-gated mesoporous nanoparticles-based analysis is a new platform for mutation detection that has the advantages of sensitivity, rapidity, accuracy, and convenience. A specific mutation in β-Thalassemia (IVS-110), as one of the most prevalent inherited diseases in several countries, was used as model mutation sequence in this study.

ÖZET

PROB-GİRİŞLİ SİLİKA NANOPARTİKÜLLER TARAFINDAN BİR TALASEMİ NOKTA MUTASYONUNU GENOTİPLENDİRME

β-talasemi, anemiye yol açabilen kalıtsal bir kan hastalığıdır. Hastalığın nedeni, beta hemoglobin adı verilen alt birimlerden birini üreten hemoglobin (HBB) geninde mutasyon (lar) olduğu bilinmektedir. HBB genindeki mutasyonlar, anormal hemoglobin protein yapısına ve dolayısıyla oksijen taşıma kapasitesine yol açan beta-hemoglobin üretimini azaltabilir veya yok edebilir. Bu nedenle, kandaki az sayıda kırmızı kan hücresi, kişinin hemoglobin üretme yeteneği ve ilişkili anemi komplikasyonlarına neden olur.

Ortak mutasyonların moleküler tespiti için basit, güvenilir ve hızlı yaklaşımların geliştirilmesi, Talasemi de dahil olmak üzere genetik hastalıkların önlenmesi ve erken teşhisi için önemlidir. Hassasiyet, hızlılık, doğruluk ve kolaylık avantajlarına sahip olan oligonükleotid-girişli, mezo-gözenekli nanoparçacıklara dayalı analiz; mutasyon tespiti için yeni bir platformdur. Bu çalışmada, birçok ülkede en yaygın görülen kalıtsal hastalıklardan biri olan β-Talasemi'de spesifik bir mutasyon olan IVS-110; model mutasyon dizisi olarak kullanılmıştır.

TABLE OF CONTENTS

LIST OF FIGURES

LIST OF TABLES

LIST OF SYMBOLS/ABBREVIATIONS

AFM	Atomic Force Microscopy
APTES	(3-Aminopropyl)triethoxysilane
BET	Brunner Emmet and Teller
CBB	Coomassie Brillant Blue
DLS	Dynamic Light Scattering
DNA	Deoxyribonucleic acid
FTIR	Fourier Transform Infrared Spectroscopy
Hb	Hemoglobin
HBB	Hemoglobin subunit β gene
MCM-41	Mobile Crystalline Material
PBS	Phosphate Buffer Saline
PCR	Polymerase Chain Reaction
RNA	Ribonucleic acid
SEM	Scanning Electron Microscopy
SNP	Single Nucleotide Polymorphism
TEM	Transmission Electron Microscopy
XPS	X-Ray Photoelectron Spectroscopy

1. INTRODUCTION

1.1. HEMOGLOBIN

Hemoglobin (Hb) is a tetrameric protein which comprise of four subunits and one heme group for per subunit [1]. It is approximately 6.4 nm in diameter and has 64,500 dalton of molecular weight [2]. Hb molecule consists of globin protein and heme group. Globin has four polypeptide chains and a heme group binds to each chain. This provides binding of oxygen to hemoglobin molecule by binding to heme group [3]. After heme group and globin chains are synthesized in different places of cells, they are combined to form hemoglobin molecule (Figure 1.1) [4].

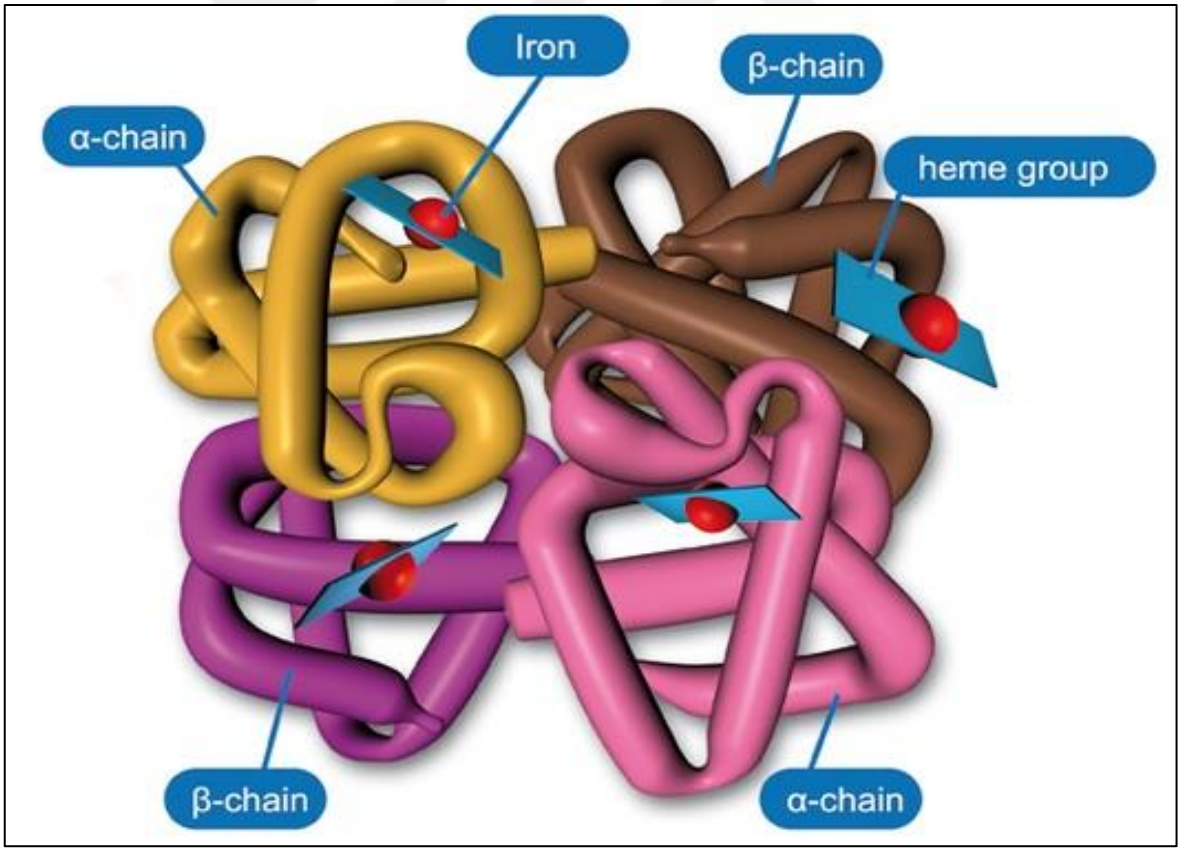

Figure 1.1. The structure of Hb molecule [5]

The Hb protein, located in erythrocytes, transports oxygen from lung to tissues via oxygen binding to heme group. Also, hemoglobin transports carbondioxide and proton from tissues to lung. This signifacant function provides buffering action of the circulating blood and also give the red color of blood [6]. Therefore, hemoglobin has a vital importance in order to maintain the function of tissues and organs.

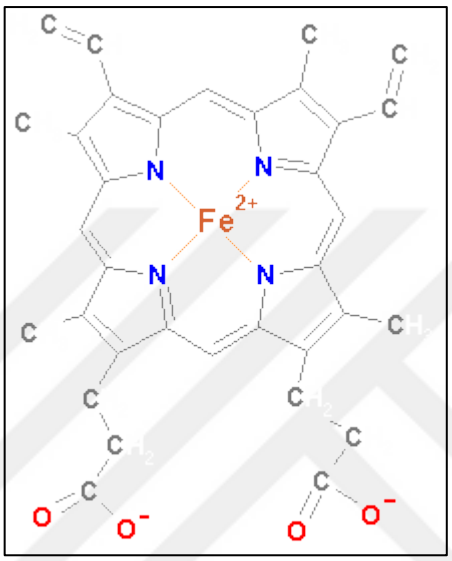

Figure 1.2. Molecular composition of Heme group [7]

Heme group composed of four pyrrole rings, with ferrous (Fe^{+2}) in the middle and side chains, linked together by methyl bridge is the same in the all hemoglobin types (Figure 1.2) [3].

Erythroblasts can synthesize six different polypeptide chains which are alpha, beta, gamma, delta, epsilon, and zeta. α-like subunits, β-like subunits and tetramer compositions of different types of hemoglobins shown in Table 1.1 [6].

Table 1.1. The types of human hemoglobin and their subunits

Hemoglobin	α-like subunit	β-like subunit	Tetramer Composition
Hb A	α	β (Beta)	$\alpha_2 \beta_2$
Hb A_2	α	δ (Delta)	$\alpha_2 \delta_2$
Hb F	α	Gγ, Aγ	$\alpha_2 \gamma_2$
Hb Gower-2	α	ε (Epsilon)	$\alpha_2 \varepsilon_2$
Hb Gower-1	ζ (Zeta)	ε (Epsilon)	$\zeta_2 \varepsilon_2$
Hb Portland	ζ (Zeta)	γ (Gamma)	$\zeta_2 \gamma_2$

Embryonic hemoglobins are Gower-1, Gower-2 and Portland which contain different epsilon and zeta chains. During the normal development of human, Hb Portland, Hb Gower-1, Hb Gower-2 are found in embryonic period, Hb F (or fetal Hb) along fetal stage, Hb A (or adult Hb) and also little amounts of Hb A_2 are found in adults [8]. Hb F constitutes majority of Hbs after 8th week of gestation. There is about 90% Hb F in the total hemoglobin after 6th month of gestation. Then, rate of Hb F decreases and, synthesis of Hb A ,which is adult hemoglobin, starts. In adults, there are at least 96% Hb A, 2,5-3% Hb A_2 and less than 1% Hb F.

Embryonic globin synthesis occurs in the period from 3rd week of pregnancy to 8th week. After about 5th week of pregnancy, hematopoiesis continues in main location which is fetal liver. As erythropoiesis begins in liver, fetal erythrocytes occur and Hb synthesis is seen starting from 12th week. Red cell production passes slowly from fetal liver to bone marrow from 18th week of pregnancy to the birth [9]. In embryonic, fetal and adult life it is observed that as one of globin synthesis decreases, the other starts to increase (Figure 1.3) [2].

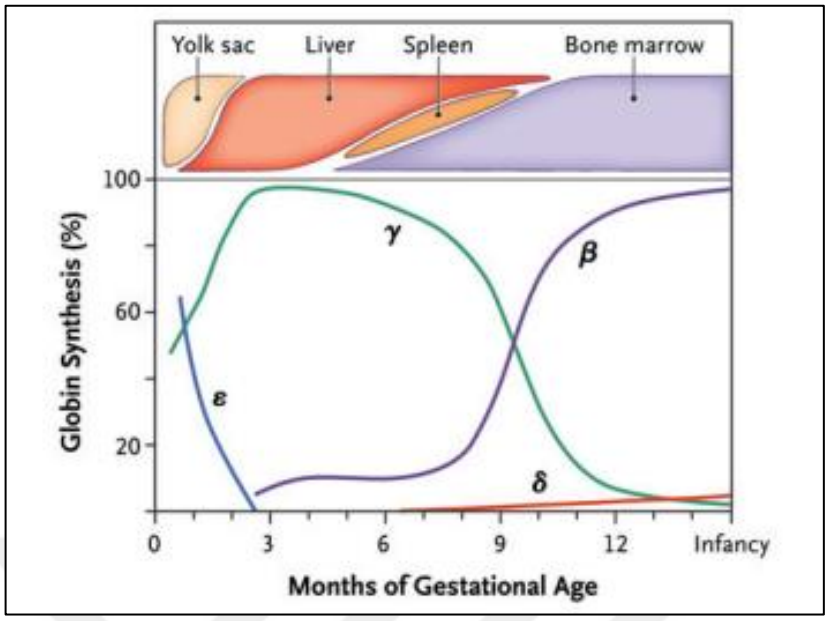

Figure 1.3. The stages of globin chain synthesis [10].

The genes which synthesize different globin chains are grouped into two set as alpha-like (ζ2–Ψζ1–Ψα2–Ψα1-α2-α1-θ) and beta-like (ε-Gγ-Aγ-Ψβ-δ-β). alpha-like genes are found in chromosome 16 and beta-like genes on chromosome 11. In addition, α polypeptide chains consist of 141 amino acids, β polypeptide chains consist of 146 amino acids. The differences in Hb molecule occur as a result of amino acid changes on globin chains. These changes are directly relevant with genes which encode Hb molecule (Figure 1.4) [11] .

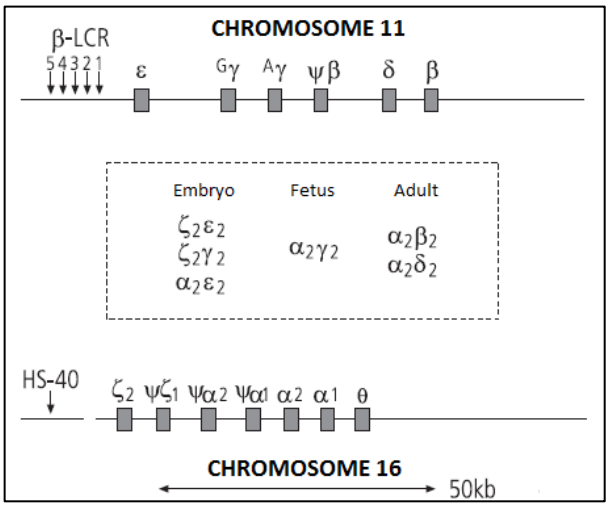

Figure 1.4. Hb gene clusters on chromosome 11 and 16 [11].

1.1. THALASSEMIA

Hemoglobinopathies are one of the most important inherited disease which caused by defects in globin gene product [12]. Mostly, substitution of a single amino acid in the sequence of globin gene results in this disorder [13]. One of the most prevalent hemoglobinopathy is Thalassemia.

Thalassemia is a genetic disease caused by mutations in the globin gene resulted in low amount or lacking one of the globin subunits [14]. It is autosomal recessive which means not related to sex chromosomes, and therefore the disease can be seen equally in the both sex (girls and boys) [2].

Thalassemia has two types: α-thalassemia and β-thalassemia. In α-thalassemia, α subunit of the globin chain synthesis is low or absent. While the mild subgroups of α-thalassemia are silent carrier and α-thalassemia carrier, the most important subgroups are HbH disease and Hb Bart's Hydrops fetalis. In β-thalassemia, just like α-thalassemia, β subunit of the globin synthesis is low or absent. The subgroups of β-thalassemia are thalassemia minor, thalassemia intermedia and thalassemia major. The common feature of all thalassemia types is the imbalance in globin chain synthesis which comprises hemoglobin tetramers (Figure 1.5.) [2, 15].

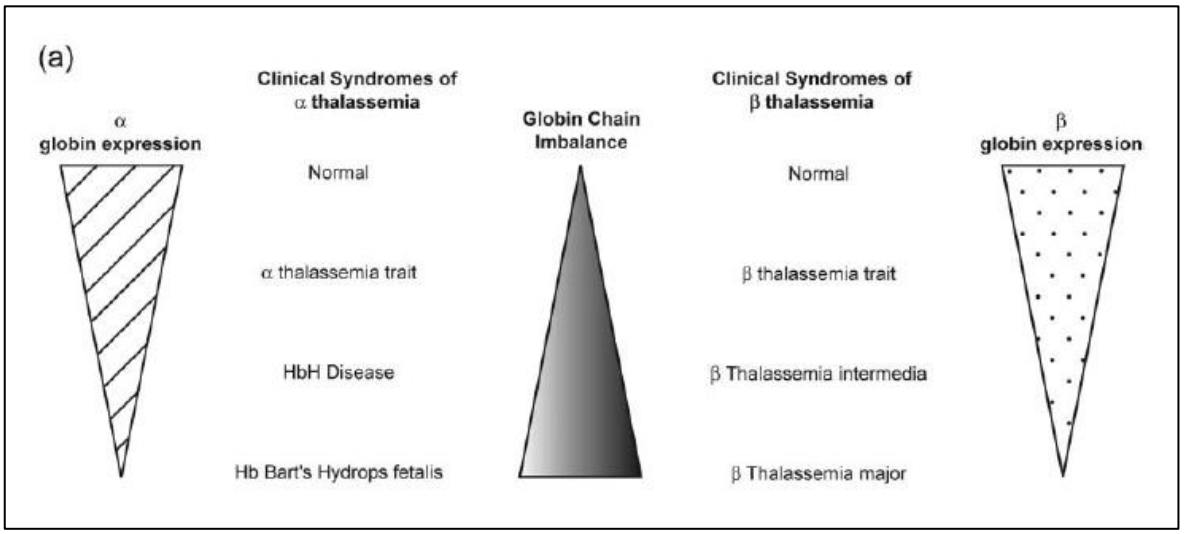

Figure 1.5. Clinical Syndromes of Thalassemia Types [15].

1.1.1. Alpha Thalassemia

Alpha-like genes located on short arm of chromosome 16p13.3 and normaly two genes found in each homologous chromosomes, so totally there are four. Two of them come from mother, the other two come from father. α-genes on the same chromosome is named as alpha 2 (α2) ve alpha 1 (α1) by the direction of 5′→3′[2]. The most common pathology of α-thalassemia is gene deletions [16]. α-thalassemia is not rare genetic disease in contrast to this, it is known by people and one of the most prelavant genetic abnormalities [17]. Normal α genotype is indicated as αα/αα. In α-thalassemia, one, two, three or four α globin genes can be affected.

α^{+}-thalassemia (silent thalassemia or α-thalassemia-1) involves deletion of one α globin genes.Genotype is shown as α-/αα. Since its phenotype is silent, there are no clinical outcomes [18].

α^{0} -thalassemia (α-thalassemia carrier or α-thalassemia-2) involves deletion of two α-globin chain genes. Genotype is shown as (α-/-α) or (--/αα). Clinically mild anemia is observed. The most common form of this anemia type is homozygous of 3,7 kb deletion which is shown as $\alpha^{3,7}$/ $\alpha^{3,7}$. There are same hematologic findings in β-thalassemia carriers, too. After birth Hb Barts is observed but it disappears six months later [18].

Hemoglobin H disease results from inactivation of 3 α globin genes due to different mutations or deletions. In this condition, β_4 tetramer is formed and it is known Hb H. The people, who have Hb H disease, generally have hemolytic anemia, hypochromia and marked microcytosis.

The most serious type of α-thalassemia is Hb Bart's Hydrops Fetalis Syndrome. In this disease, four α globin genes are inactive and therefore α globin chains cannot be synthesized [19]. In literature, alive patient due to this syndrome has rarely encountered. In addition, skeletal and urogenital system abnormalities, severe neurological disorders are reported [20,21].

1.1.2. Beta Thalassemia

The Hemoglobin subunit β gene (HBB) is located in the p15.4 region on the short arm of the 11th chromosome. The order of the genes is 5'-epsilon -- gamma-G -- gamma-A -- delta -- beta--3' in the beta-globin cluster. The β-globin gene carries the necessary information and encode 146 amino acids found in the β-globin chain about 1.8 kb which includes 3 exons, 2 introns and 5 'and 3' regulatory regions [22]. Mutations in the beta globin genes resulted in reduced (β^+) or absent (β^0) synthesis of the beta globin chains. When β-globin synthesis is not complete, β^0 thalassemia occurs. When β-globin synthesis is leastwise, β^+ thalassemia occurs. Beta Thalassemia are classified into three types; thalassemia major, thalassemia intermedia and thalassemia minor.

1.1.2.1. Thalassemia Major

Thalassemia major is the basis of the chronic hemolytic anemia clinic which is due to accumulation of α-globin chains versus β-globin chains lacking or not synthesized at all, and due to low erythrocyte hemoglobin. In babies born with thalassemia major, it is asymptomatic due to high amount of HbF in the first months and symptoms become symptomatic when HbA starts to take its place for about 4-6 months. Patients with β-thalassemia major begin the treatment of thalassemia in the first year of their life and consequently need regular blood transfusion throughout life.

1.1.2.2. Thalassemia Intermedia

It can be asymptomatic until the adult life but clinically characterized patients are usually diagnosed between the ages of 2 to 6 years. Thalassemia intermedia patients can continue their lives without blood transfusion or they may need it occasionally. The symptomatic distinction between Thalassemia Major and Thalassemia Intermedia is not clear. Therefore, hematologic, genetic and molecular instrumental techniques is necessary to distinguish Thalassemia Major and Thalassemia Intermedia for appropriate treatment [23].

1.1.2.3. Thalassemia Minor

Carriers with a single defective β-globin gene live an asymptomatic life. Their physical examinations are natural and they can be diagnosed by routine blood counts or by researching family history stories [24].

1.2. NUCLEIC ACID BASED DIAGNOSTIC SYSTEMS

Every living organism have unique nucleic acid sequences and these are used as a target to identify the organisms and diagnose the various diseases. Nucleic acid based diagnostic methods have an important place in clinical laboratories to analyze sequence variations and expression of deoxyribonucleic acid (DNA) and ribonucleic acid (RNA). These methods can be separated in to two groups: i) amplification based and ii) direct detection. In amplification based methods in vitro amplification is used in order to increase the amount of the target DNA or RNA sequence. In contrast, direct detection methods use a hybridization probe to target sequence directly.

Polymerase chain reaction (PCR), transcription-based amplification, and strand displacement amplification are some of the amplification techniques. The common feature of these methods is that they all use single or multiple enzymes for nucleic acid synthesis to obtain copies of target sequence [25].

1.3. SNP AND DETECTION PLATFORMS

The most abundant form of genetic variation is the single nucleotide polymorphisms (SNPs) which are changes in the sequence of particular genes. SNPs cause many genetic diseases including malignant ones [26,27,28]. Every human carries the same base residue on both chromosomal homologs at the great majority of genomic sites which is approxiamately 99%. Diversity among humans and also differences in disease susceptibility are coded by the remaining. Major part of these DNA variants are composed of SNPs which defined as genome positions at which there are two distinct nucleotide residues (alleles) that each appears in a significant portion of the human population. They occur approximately once in every 300-1000 nucleotides [29,30, 31,32]. It is estimated that there are 10 million SNPs in human genome [33].

In humans, “Hemoglobinopathy” and “thalassemia” are the most common single gene disorders. About 7% of the world population carries a globin gene mutation, and it is inherited as an autosomal recessive trait in the vast majority of cases. Inherited abnormalities of the hemoglobin tetramer can be classified into two: structural anomalies of the hemoglobin chains and molecular defects in the synthesis of hemoglobin chains. Globin gene mutations are referred as ‘hemoglobinopathy’ and then some of them are defined as ‘thalassemia’ [32,34].

Over 1,200 different mutant alleles have been characterized at the molecular level to date. Each country also has its own mutational spectrum of Hb variants and thalassemia mutations. In Turkey where located in Mediterranean region, IVS–1–110 (G>A) is the most frequently observed mutation. The rate of β thalassemia carriers with abnormal hemoglobins is 3,5% in Aegean Region; especially around Denizli, according to the records of Department of Public Health, Denizli. In our country, the incidence of β thalassemia is 2,1% and this rate can be different due to regions. A prevention program is carried out for hemoglobinopathies in our country by the Ministry of Health of Turkish Republic. The fundamental aim is to determine the possible risks and to help healthy babies to be born [35,36,37,38]. Since the incidence is quite high and easy routine tests are necessary, cheap and fast molecular screening methods are required for the detection of hemoglobinopathies and other SNPs.

2. MATERIALS

2.1. INSTRUMENTS

The instruments used in this study are as follows:

- Incubator with shaker (Incubator 1000, Unimax 1010, Heidolph)
- Centrifuge (5810R, Eppendorf)
- Vortex (MX-S, SciLogex)
- AccuBlock Digital Dry Bath (Labnet)
- Synergy H1 microplate reader (BioTek)
- UV Spectrophotometer (Agilent)
- Sonicator
- Balance (Ohaus)
- Ultrapure Water System (Direct Q Millipore)
- Thermal Cycler (Biorad T100)
- ENDURO™ GDS Gel Documentation System (Labnet)

2.2. EQUIPMENTS

The laboratory equipments used in this study are as follows:

- Micropipettes 1000, 200, 100, 10 and their tips (Eppendorf)
- Polypropylene centrifuge tubes, 50 ml, 15 ml, 2 ml, 1 ml, 0.5 ml
- Cuvettes
- Beakers

2.3. CHEMICALS

- MCM-41 type (hexagonal) mesoporous silica particles (Sigma-Aldrich)
- Phosphate Buffered Saline (PBS)

- Fluorescein Sodium Salt (CAS number: 518-47-8) (Sigma-Aldrich)
- 99,8% Acetic Acid Glacial (Sigma-Aldrich)
- Ethanol absolute (Sigma-Aldrich)
- (3-Aminopropyl)triethoxysilane (APTES) (Sigma-Aldrich)
- Streptavidin magnetic beads

The oligonucleotides were synthesized by Sentromer (Istanbul). The DNA sequences used in this study were listed in Table 2.1.

Table 2.1. DNA sequences used in this study.

NAME	SEQUENCE
IV110R	5'-Bio-CACCAGCAGCCTAAGGGTG-3'
IV110F	5'-TGATAGGCACTGACTCTCTCTG-3'
TPROBE	5'-CTATTAGTCTATTTTCCCACCCTTAG-3'
TCOMP	5'-CTAAGGGTGGGAAAATAGACTAATAG-3'
NPROBE	**5'**-CTATTGGTCTATTTTCCCACCCTTAG-3'
NCOMP	**5'**-CTAAGGGTGGGAAAATAGACCAATAG-3'

2.4. KITS AND SOLUTIONS

- DNA Isolation Kit (Sigma GenElute)
- PCR Kit (NEB Onetaq)

3. METHODS

3.1. CHARACTERIZATION OF MCM-41 PARTICLES

The MCM-41 type mesoporous nanoparticles were characterized by Scanning electron microscopy (SEM), Transmission electron microscopy (TEM), Dynamic Light Scattering (DLS), Brunnauer, Emmett and Teller (BET) and Atomic Force Microscopy (AFM) analysis as explained below. Amino grafted particles were prepared, and quantified with Coomassie Brillant Blue assay. Then, Fourier Transform Infrared Spectroscopy (FTIR) was performed.

3.1.1. SEM Analysis

SEM is a technique of nanoscale image formation by focusing electron beams on the sample. It is useful to image surface topography of nanoparticles. The analysis of MCM-41 samples were obtained in a Zeiss (EVO LS 10) microscope under high vacuum conditions (3000 Pa) (Yıldız Teknik University, MERKLAB).

3.1.2. TEM Analysis

TEM is a technique used to observe morphological, compositional and crystallographic information about samples. MCM-41particles were prepared by ultrasonication of powders in ethanol for 5 min and drying of a droplet of suspension on a standard holey carbon TEM grid. TEM analysis was carried out on Titan 60-300 electron microscope (FEI, The Netherlands) operating at 300 kV in TEM mode (CIC nanoGUNE, Donostia-San Sebastián, Spain).

3.1.3. BET Analysis

BET method was used to determine internal and external surface area and pore sizes in a Quantachrome BET analyser (Yıldız Teknik University, MERKLAB). Around 100 mg of MCM-41 particles were used in the analysis.

3.1.4. DLS Analysis

DLS is a technique used for determining size of nanoparticles in a solution. Photons scatter when hit the surface of nanoparticles and interact with the surface electrons. Rayleigh scattering is defined as the intensity of scattered light when a laser beam interact with colloidal spherical particles display Brownian motion. Zeta potential is a measure of its surface charge. The size of the particles was determined by a Zetasizer ZEN 3600 Nano-ZS, (Malvern Instruments, Worcestershire, UK) (Yıldız Teknik University, MERKLAB). About 1 mg MCM-41 particles were suspended in PBS buffer and analyzed to obtain intensity versus diameter size graph. The hydrodynamic diameter of silica particles were automatically obtained from software.

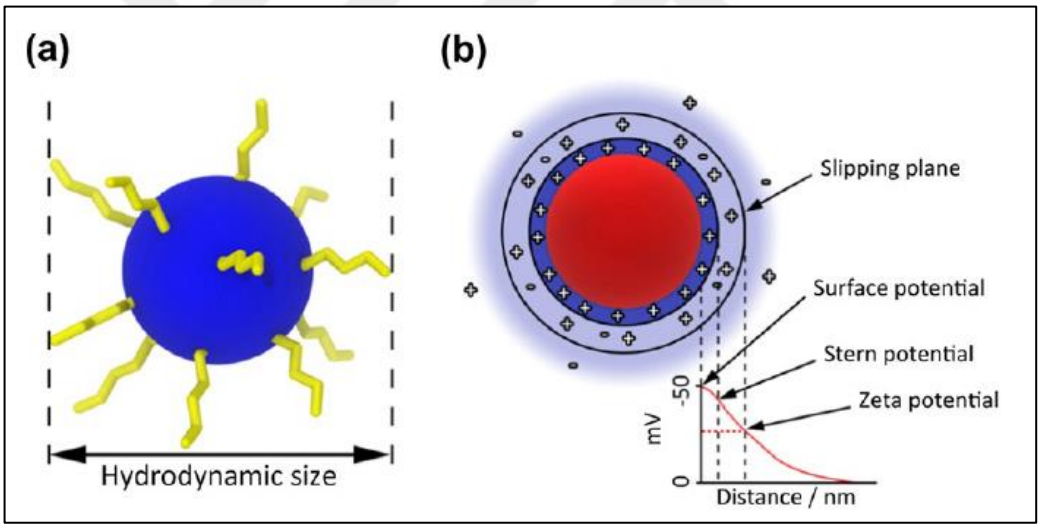

Figure 3.1. a) Hydrodynamic size of a modified nanoparticle, b) the double layer on a negatively charged particle.

3.1.5. AFM Analysis

AFM is another technique for nanometric imaging of non-conductive materials. A nanometer sharp tip mounted on a cantilever is dawn across sample and the changes in force is used to obtain an image. MCM-41 particles were analyzed with an AFM (Nanomagnetics Instruments, Ankara).

3.1.6. Amino Grafting and Quantification

Amino-functionalized SiO_2 NPs were prepared according to a previously reported procedure [39]. 50 mg of MCM-41 powder was stirred with 1 ml of 95% ethanol containing 5% 1 mM of acetic acid for 1 hour at room temperature. 3% (3-Aminopropyl)triethoxysilane was added and followed by overnight incubation under mixing. Three-fold washing with 1X PBS during centrifugation (14000 rpm, 5 min.). This tube was labeled as B1.

3.1.7. FTIR Analysis

FTIR were used to determine amine bond formation on the surfaces of SiO_2 nanoparticles. A spectrum scan of wavelengths between 650 cm^{-1} and 4000 cm^{-1} were obtained by a Perkin Elmer spectrum 100 (Yıldız Teknik University, MERKLAB) from 1 ml of nanoparticle samples in PBS.

3.2. PREPARATION OF PROBE-GATED SILICA NANOPARTICLES

3.2.1. Loading with Fluorescein

B1 labeled tube was divided to two tubes including 500 µl in each and were labeled as T and S. 5 µl of Fluorescein solution was added to T and S , then tubes were placed into sonicator at 25°C for 15 minutes. After that, they were left for overnight incubation on the shaker. The fluorescein solution was prepared by weighing 3,5 mg Fluorescein Sodium Salt and mixing with 1 ml of PBS buffer (0.01 M phosphate buffered saline; NaCl-0.138 M; KCl-0.0027 M; pH 7.4). This Fluorescein solution was stored at 4°C.

3.2.2 Capping with Synthetic Probes

The amino-modified nanoparticles (1 mg) were loaded with fluorescein after an overnight incubation period in 100 µM fluorescein solution and used for interacting with 1 µM thalassemia (Tprobe) or normal (Nprobe) sequence oligonucleotides (Table 2.1). The

particles were then washed thoroughly 3 times with PBS buffer. Fluorescence intensity of particles were measured and the loading amount was calculated by using a standard calibration curve. The DNA absorbance (260 nm) of incubation solution was measured before and after incubation procedure. Then, the capping oligonucleotide immobilization amount was calculated.

3.2.3 Release Experiments with Synthetic Probes

B1 labeled tube was prepared as above. Then, it was divided to two tubes labeled as B2. Fluorescein was loaded again as above. After overnight incubation, 100 µl was taken from B2, 100 µl PBS and 2 µl TP was mixed in a tube labeled as C1. Also, into the other tube C2, 2 µl NP was added as different from C1. These tubes were incubated overnight at room temperature. After that, 10 µl of mixtures were taken into another 2 tubes ($C1_{TPcp}$ & $C1_{NPcp}$) from C1 and 2 tubes ($C2_{TPcp}$ & $C2_{NPcp}$) from C2. 100 µl of PBS was added to tubes and they were centrifuged at 14000 rpm for 1 minute. Supernatants were removed, PBS was added and the solution was centrifuged. This step repeated twice. Cp mixtures were prepared by adding 10 µl Cp (TP or NP) into 1500 µl PBS.

100 µl Cp mixture was added to tubes according to the following procedure. First Cp mixture was centrifuged at 14000 rpm for 1 minute. 50 µl supernatant was collected and put into 96 well plate. 50 µl from Cp mixture was added tubes, after 1 minute incubation, the mixture was centrifuged at the same conditions. Then, 50 µl from supernatants was put into 96 well plate. 50 µl from Cp mixture was added into tubes. The same procedure applied for the incubation times; 2, 5, 10, 15, 30 minutes and 1, 2, 3, 4, 24 hours.

B1= 50 mg MCM-41 + 1 ml (95% EtOH+5% Acetic Acid) + 30 µl 3-Aminopropyl-trimethoxysilane
B2= 500 µl form B1 + 5 µl Fluorescein solution
C1= 100 µl from B2 + 100 µl PBS + 2 µl TP
C2=100 µl from B2 + 100 µl PBS + 2 µl NP
$C1_{TPcp}$ = 10 µl C1 + 100 µl (TPcp mixture with PBS)
$C1_{NPcp}$ =10 µl C1 + 100 µl (NPcp mixture with PBS)
$C2_{TPcp}$ =10 µl C2 + 100 µl (TPcp mixture with PBS)

$C2_{NPcp}$ =10 µl C2 + 100 µl (NPcp mixture with PBS)

C1 and C2 were prepared as above. Different concentrations of TP_{cp} and NP_{cp} were prepared and then, $C1_{TPcp}$ and $C2_{NPcp}$ were prepared according to the following tables.

Table 3.1. Preparation of $C1_{TPcp}$

$C1_{TPcp}$			
CP Concentration	C1	PBS	TPcp
1 µM	10 µl	90 µl	1 µl
500 nM	10 µl	90 µl	0,5 µl
100 nM	10 µl	80 µl	10 µl
1 nM	10 µl	90 µl	1 µl
500 pM	10 µl	90 µl	0,5 µl
100 pM	10 µl	80 µl	10 µl
1 pM	10 µl	90 µl	1 µl
500 fM	10 µl	90 µl	0,5 µl

Table 3.2. Preparation of $C2_{NPcp}$

$C2_{NPcp}$			
CP Concentration	C1	PBS	NPcp
1 µM	10 µl	90 µl	1 µl
500 nM	10 µl	90 µl	0,5 µl
100 nM	10 µl	80 µl	10 µl
1 nM	10 µl	90 µl	1 µl
500 pM	10 µl	90 µl	0,5 µl
100 pM	10 µl	80 µl	10 µl
1 pM	10 µl	90 µl	1 µl
500 fM	10 µl	90 µl	0,5 µl

At room temperature, it was incubated for 15 minutes and centrifuged with 14000 rpm for 5 minutes. Then, 50 µl supernatant was loaded into 96-well plate, 50 µl PBS loaded as blank, and measured by fluorescence spectrophotometry.

3.3. PREPARATION OF REAL SAMPLES

3.3.1 Isolation of genomic DNA from blood samples

20 µl of Proteinase K solution was put into 1,5 ml microcentrifuge tube containing 200 µL of the whole blood sample, vortexed and then, 200 µL of Lysis Solution was added to the sample and vortexed throughly for 15 seconds. It was incubated at 55°C for 10 min. 500 µL Column Preparation Solution was added to GenElute Miniprep Binding Column and centrifuged at 12,000xg for 1 min. The liquid was discarded the flow-through. 200µL of ethanol was put into the lysate (sample) and vortexed for 5-10 seconds. The entire contents of the tube was transferred into the column by using wide bore pipette tip. Then it was centrifuged at 6500xg for 1min. The liquid in the collection tube was discarded the flow-through and then placed the column in the collection tube. 500µL of Prewash solution was added to the column and centrifuged for 1 minute at 6500x*g*. The liquid in the collection tube was discarded the flow-through and then placed the column in the collection tube. 500µL of Wash Solution was added to the column and centrifuged for 3 minute at 12000x*g* to dry the column. The liquid was discarded the flow-through and centrifuged for 1 additional minute at 12000x*g*. Collection tube was discarded and then the column was placed in a new collection tube. 200 µL of the Elution Solution was put directly into the center of the column. To increase the elution efficiency, incubation was done for 5 minutes at room temperature. Centrifugation was applied for 1 minute at 6500x*g* to elute the DNA. The column was discarded and the supernatant containing genomic DNA was kept and stored at -20°C.

3.3.2. PCR Amplification and Gel Electrophoresis

All PCR reactions were performed in a total volume of 100 µl, with 200 nM of primers 2,5 mM of MgCl2, 10 µM of dNTP, 10x buffer (200 mM Tris pH 8.4, 500 mM KCl) and 2.5

units of Taq polymerase. The PCR reactions were heated at 94 °C for 2 min in order to completely denature the template, followed by 35 rounds of PCR, with 45 s of denaturation at 94 °C, 45 s of annealing at 63 °C, and 45 s of elongation at 72 °C. A final extension step was performed at 72 °C for 5 min. Double-stranded PCR products were checked using electrophoresis. For each sample, 10 µl was run with 2 µl of loading buffer on a 2 % (w/v) agarose gel stained with ethidium bromide and imaged by Gel Documentation System.

3.3.3. Preparation of Single Stranded DNA

60 µl from PCR products were put into 1.5 ml tubes. Then 140 µl PBS and 20 µl Streptavidin were added, vortexed and mixed for 1 hour. After that, while tubes were in the magnetic plate, supernatants were removed. 150 µl PBS was added into tube, vortexed and supernatants were removed while the tubes were in the magnetic plate. After addition of 100 µl PBS, all samples were vortexed and transferred to the pcr tubes.While tubes were on the magnetic rack, supernatants were removed, 50 µl dH_2O was added and tubes were vortexed. Tubes were placed one by one every 30 seconds into the thermal cycler which was set to 95 °C. After 2 minutes incubation, 50 µl supernatant from tubes were placed on the magnetic rack and transferred into another pcr tube. These tubes were stored at +4°C.

3.3.4. Release Experiments with Real Samples

The single stranded PCR products from blood samples were mixed with 0.1 mg of NP-FL-Tprobe or NP-FL-Nprobe particles and incubated for 20 min. at room temperature and then centrifuged at 14000 rpm for 5 minutes. Then, 50 µl supernatant was loaded into 96-well plate, 50 µl PBS loaded as blank, and release of fluorescein was measured by fluorescence spectrophotometry.

4. RESULTS

Deoxyribonucleic acids (DNA) have become a powerful tool in nanotechnology due to their unique properties such as controllable diverse conformational transitions at nanoscale or adaptable higher order structure. Single-stranded DNA probes can be used as the pore-caps for various target recognition for developing ultrasensitive universal detection systems based on mesoporous silica. Thus, sensitivity with all of the major classes of analytes can be obtained. In this study, MCM-41 type mesoporous silica nanoparticles were functionalized with amino groups on the particle surface and used for capping fluorescein molecules for bio-sensing purposes.

4.1. PREPARATION OF PROBE-GATED NANOPARTICLES

In this study, MCM-41 type mesoporous nanoparticles were first characterized to ensure the use of mesoporous and homogenous nanoparticle through the standard characterization methods. The particles, then, were functionalized with amino groups and finally capped with an oligonucleotide probe sequence.

4.1.1. Characterization of MCM-41 Particles

The morphological structure of MCM-41 were investigated with scanning electron microscopy (SEM) analysis. Figure 4.1A and Figure 4.1B are the images of typical material examples showing amorphous and spherical shape with sizes mostly less than 200 nm.used in this study. The image was collected over an area of dry samples as two-dimensional picture. Figure 4.1C and Figure 4.1D shows MCM-41 particles after they are covered with amino groups as explained in section 4.1.2. A comparison of the low magnification SEM images of amino-free and amino-covered particles revealed that smaller clusters of particles in dry form was achieved through amino modification (Figure 4.1A and Figure 4.1C). However, the individual particles were identified at similar sizes in close-up images (Figure 4.1B and Figure 4.1D). Both particles with or without amino groups were about the same morphology and sizes.

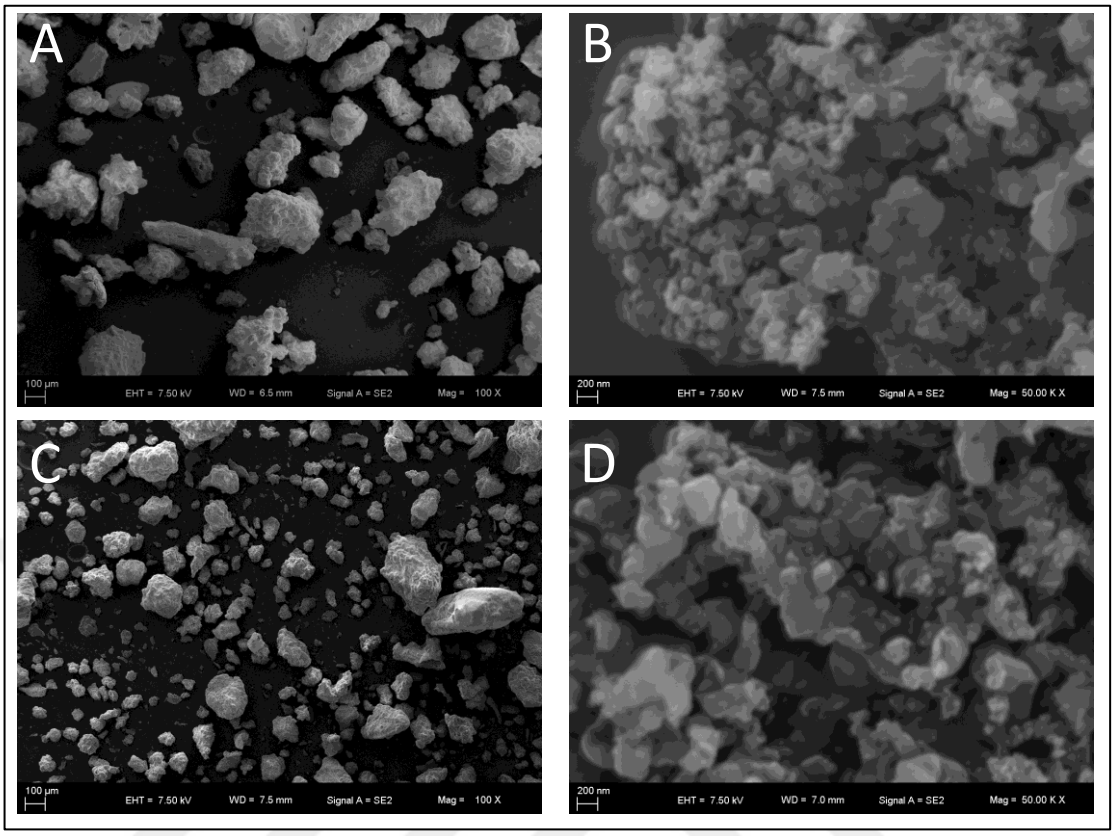

Figure 4.1. SEM micrographs of typical MCM-41 samples (A and B) and typical amino-functionalized MCM-41 samples (C and D). Magnifications are 100X or 50.000X respectively.

Similar to SEM analysis, AFM analysis indicated round particles with maximum height in a range of 20-200 nm (Figure 4.2).

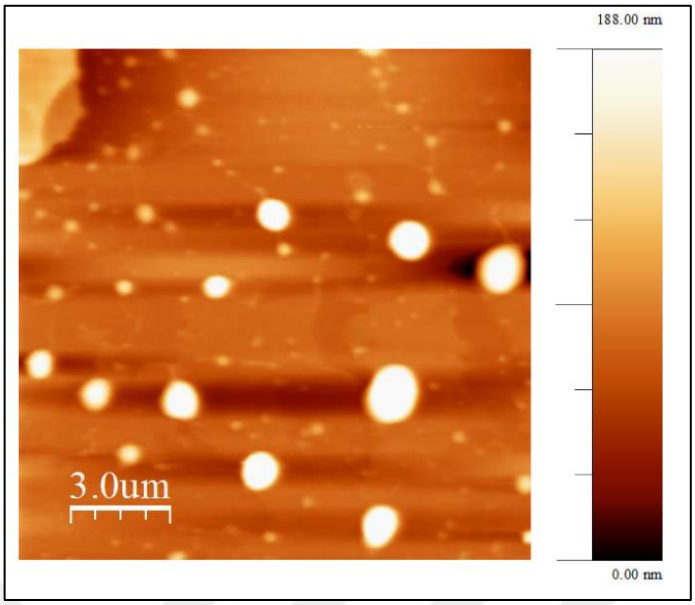

Figure 4.2. Two-dimensional AFM image of MCM-41 samples.

The sizes of the MCM-41 particles were further analysed in detail by DLS.

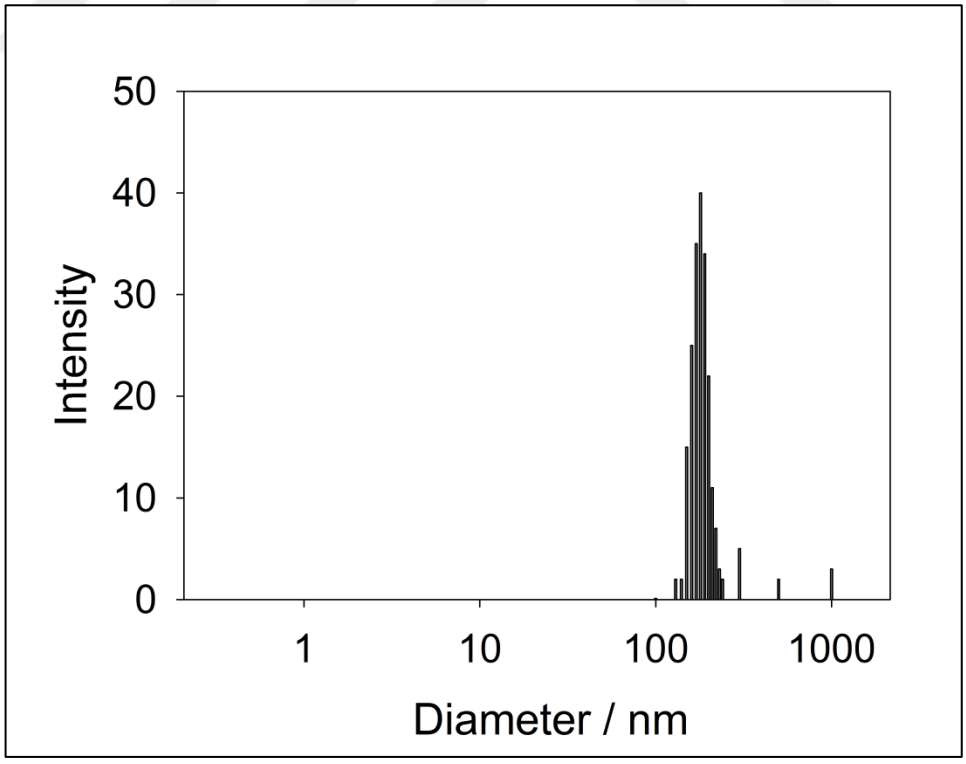

Figure 4.3. DLS analysis of a typical MCM-41 sample.

Mesoporous silica particles (MCM-41) were covered by regular hexagonal nanopores, which is typical architecture for this material (Figure 4.4)

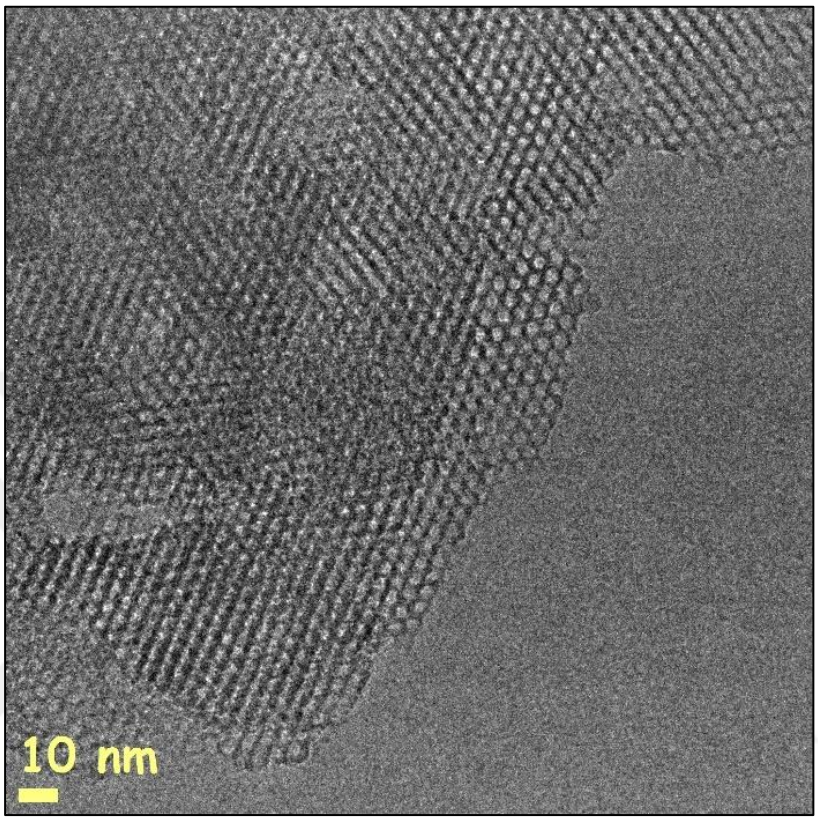

Figure 4.4. Representative TEM image for hexagonal ordered pore structure on the MCM-41 particle surface.

BET surface area analysis uses an inert gas (nitrogen) adsorption to determine the total internal and external surface area of materials [40]. The method determines uptake of nitrogen at various pressures and plots called isotherm. The analysis of isotherms can give pore size and distributions of a particle. Figure 4.5 shows that the isotherm for MCM-41 fits to main type of mesoporous particles (Type IV according to IUPAC classification). The nitrogen sorption measurements with typical inflection point at about 0.6 p/p0 indicated a mesoporous structure for the nanoparticles, demonstrating type IV isotherms. Similar pore size after APTES treatment indicated to a non-significant partial pore blocking and it can be assumed that the mesopores are still accessible for the loading of fluorescein molecules.

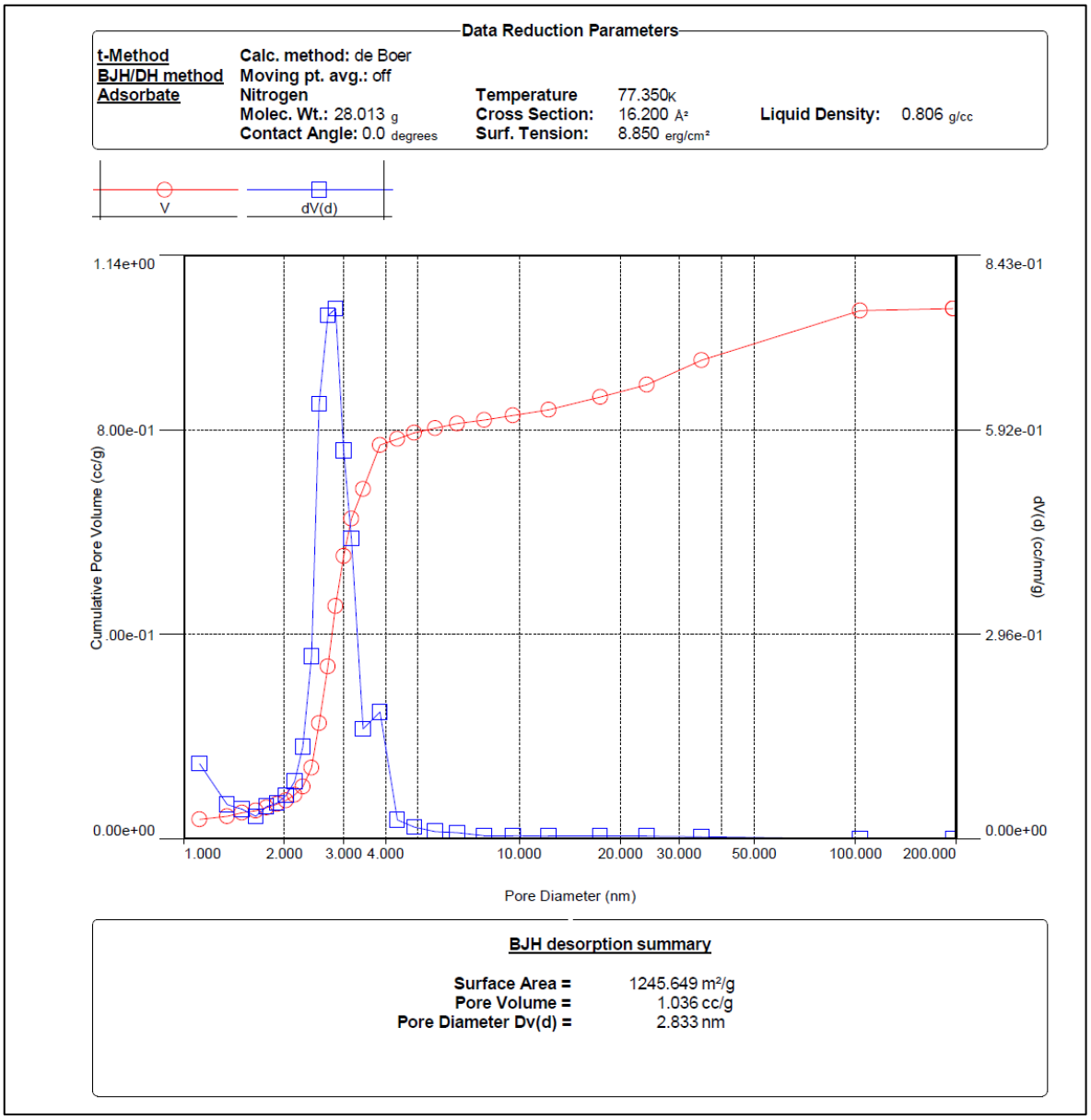

Figure 4.5. Nitrogen adsorption isotherms and pore size distribution of the particles.

4.1.2. Synthesis of Amino Functionalized MCM-41 Particles

MCM-41 particles were grafted by amino moieties through 3-aminopropyltriethoxysilane (APTES) treatment of dried SiO_2 NPs. The amination was investigated by FTIR spectroscopy and then a dye quantification method with Coomassie Brillant Blue (CBB) was used to determine the extent of amino group coverage of NPs. Figure 4.6 shows that typical bands at 690 and 1460 nm appeared after amino grafting, which can be assigned to N-H bending vibrations and N-H asymmetric bending vibrations, respectively. The

appearance of these two bands were commonly used as an evidence for presence of amino groups on the silica surfaces [41].

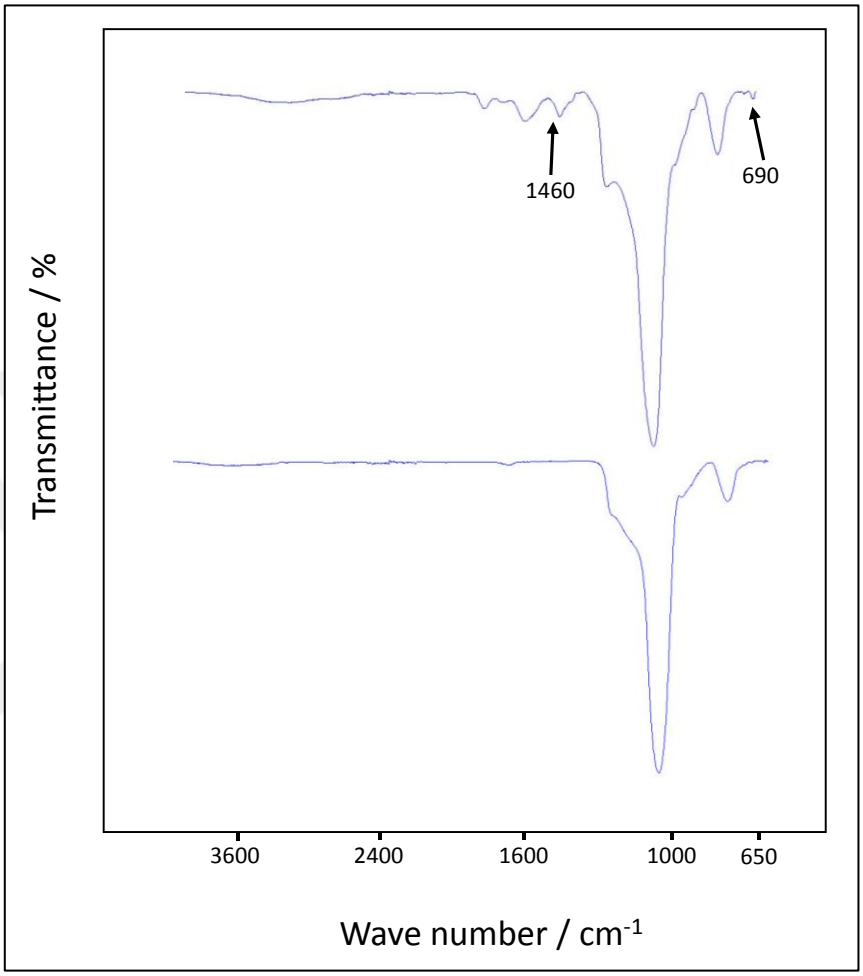

Figure 4.6. FTIR spectra of MCM-41 silica nanoparticles before (lower line) and after (upper line) amino grafting procedure.

As summarized in Figure 4.7, about 1.98 mmol amino groups per gram of nanoarticles were grafted on the nanoparticle surface. An absorbance scan at various concentrations of APTES solutions (Figure 4.7A) were obtained to draw a standard curve (Figure 4.7B). The absorbance scan of amino functionalized nanoparticles showed about 0.875 optical density at 595 nm (Figure 4.7C), which correspons to the amount of the amino groups on the nanoparticle surface. The standard curve of amino concnetration could be fitted to a linear equation (Equation 4.1).

$$OD_{595nm} = 0.0883\ [NH_2\ (mmol\ g^{-1} particle)] - 0.3499 \qquad (4.1)$$

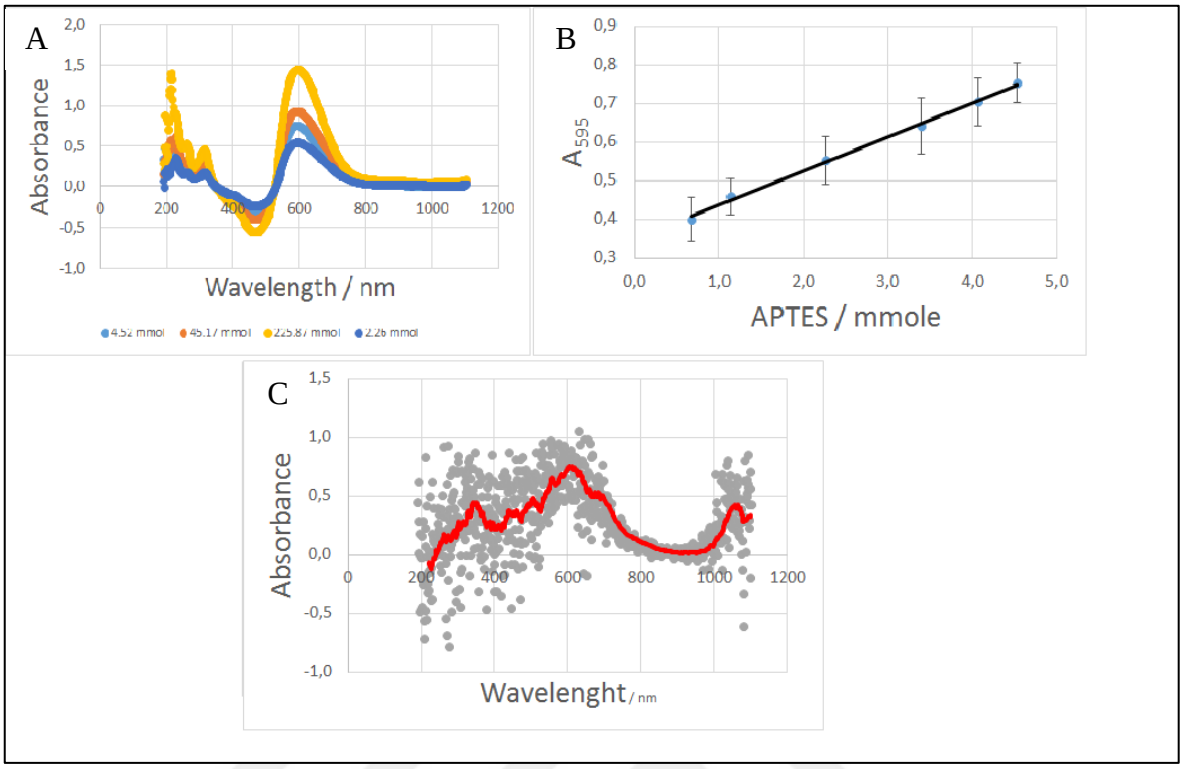

Figure 4.7. Determination of amino content of nanoparticles.

Figure 4.7 shows determination of amino content of nanoparticles after amination procedure. A) Absorbance scan of APTES molecules at various concentrations. B) The relation of absorbance versus amino amount, C) Absorbance scan of amino functionalized nanoparticles. Red line represents grey dots after negative exponential smoothing.

4.2. RELEASE ASSAY WITH SYNTHETIC PROBES

The surface of MCM-41 SiO_2 nanoparticles (NPs) were functionalized by amine moieties by treating with APTES as explained above. At the end of amine functionalization procedure, DNA capping were achieved through adsorption by electrostatic atraction between positively charged silica surface and negatively charged oligonucleotides. The silica nanoparticles were loaded with reporter fluorescein molecules and blocked by thalassemia probe ssDNA sequences (FL-NP-Tprobe) (Table 2.1). The probe sequence were designed from Human beta globulin region on chromosome 11 in The National Center for Biotechnology Information (NCBI Gene accession number: U01317.1). Figure 4.8 shows that Tprobe sequence is reverse-matching to a region of Human beta globulin

gene between 62383-62408 with only one mismatch at 62388, which is the A>G reversion in beta-thalasemmia patients with IVS-110 mutation. Nprobe seuqence has a perfect match as expected.

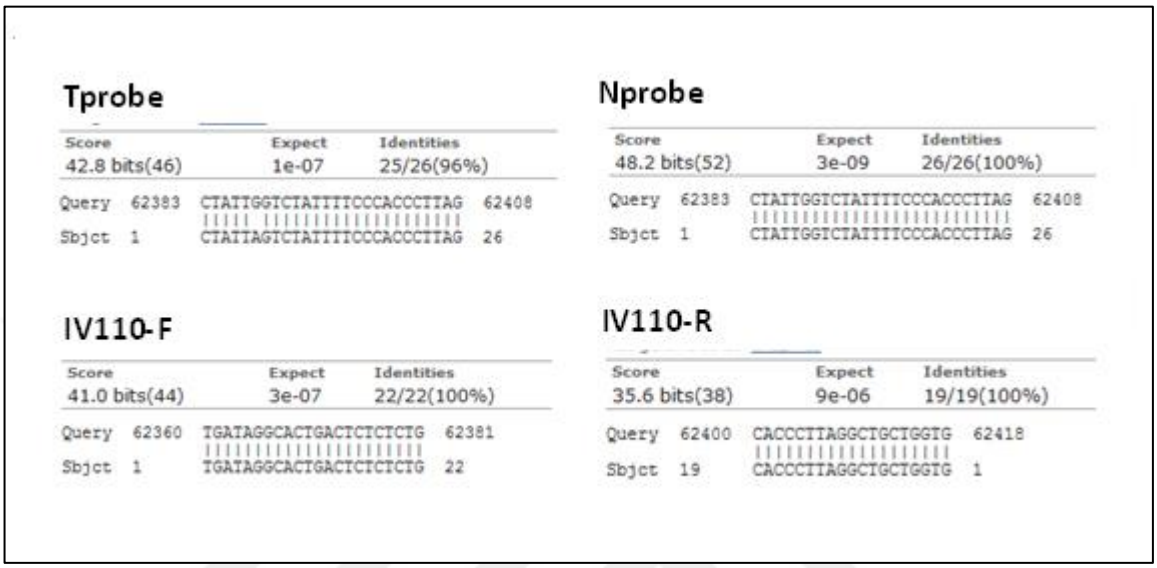

Figure 4.8**.** Probe and PCR primer locations on the Human beta globulin region of chromsome 11.

Tprobe sequences were used as cap to entrap fluorescein molecules inside the mesopores of silica nanoparticles by simple adsorption precedure to prepare FL-NP-Tprobe or FL-NP-Nprobe. A release of fluorescein occurs upon addition of complemantary sequence for thalessemi probe (Tcomp) to N-FL-Tprobe, indicating specific release based hybridization. In experiments with FL-NP-Tprobe, a minimal release of fluorescein is observed, revealing a favorable low-leakage pore-entrapment stability (Figure 4.9A, red line). Mutated target sequences caused a rapid increase in fluorescent signal when added to NP-FL-Tprobe or NP-FL-Nprobe (Figure 4.9A, green and blue lines, respectively). Figure 4.9B is a blow-up representation of early time course of release up to 60 min. The addition of thalessemia IVS-110 mutation sequence increases fluorescence signal in a linear fashion starting from 10 min. similarly, normal sequence target increases the signal. However, the addition of thalessemia target (tcomp) produced a distinctively higher signal compared to normal probe particles (NP-FL-Nprobe), starting from 5 min.

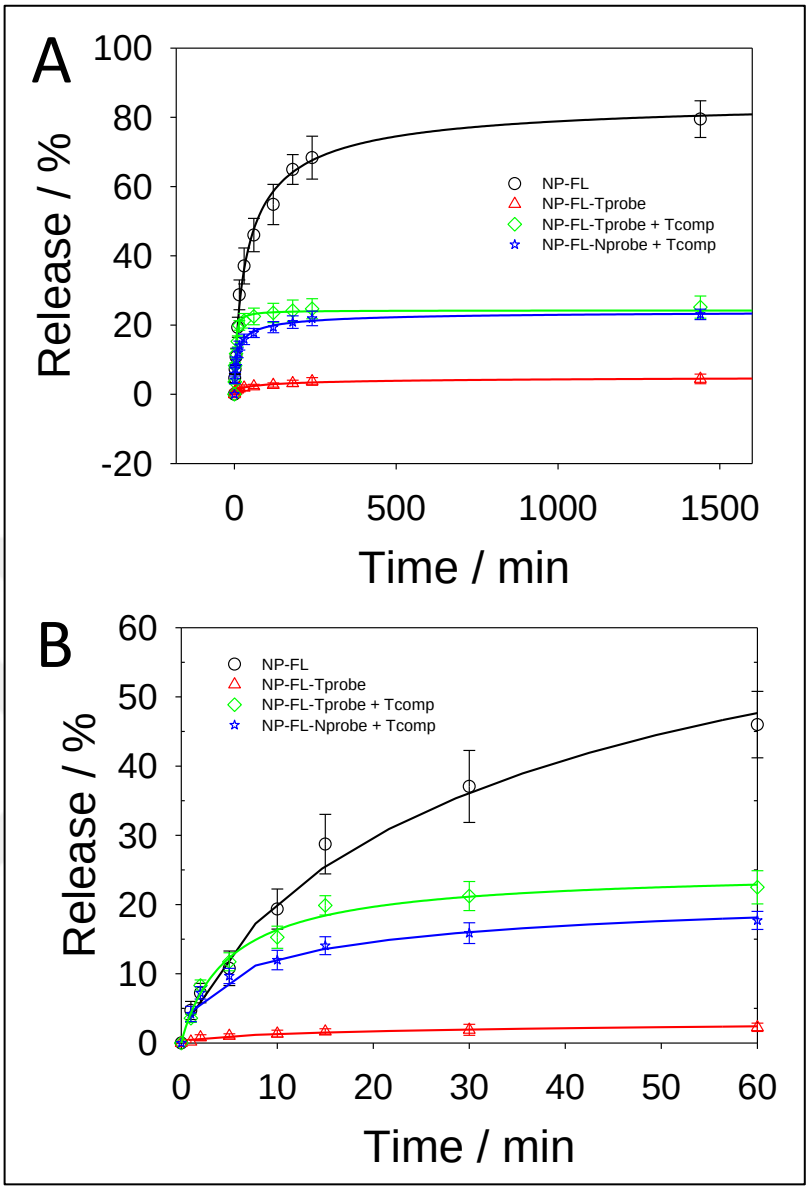

Figure 4.9. Evaluation of FL-NP-Tprobe or FL-NP-Nprobe in PBS buffer with synthetic target sequences.

The particles loaded with fluoroscein and capped with Thalessemia mutation containing oligonucleotides (Tprobe) were incubated in the buffer, to determine their stability and reporter molecule retention (red line). Addition of 1 μM of mutated target sequence Tcomp oligonucleotide were monitored for fluorescent signal to evaluate the release of reporter by the specific hybridization (green for NP-FL-Tprobe and blue lines for NP-FL-Nprobe). Black line shows fluorescein loaded silica particles without any probe or target oligos. All

the measurements were carried out in triplicate; the results show average fluorescence intensity and the error bars represent standard deviation.

On a control experiment, normal sequence target (Ncomp) were used to test the ability of the particles (NP-FL-Tprobe or NP-FL-Nprobe) to release reporter fluorescein molecules. Figure 4.10 shows that NP-FL-Nprobe particles resulted in a higher signal compared to NP-FL-Tprobe, which is the reversal of Figure 4.9 as expected.

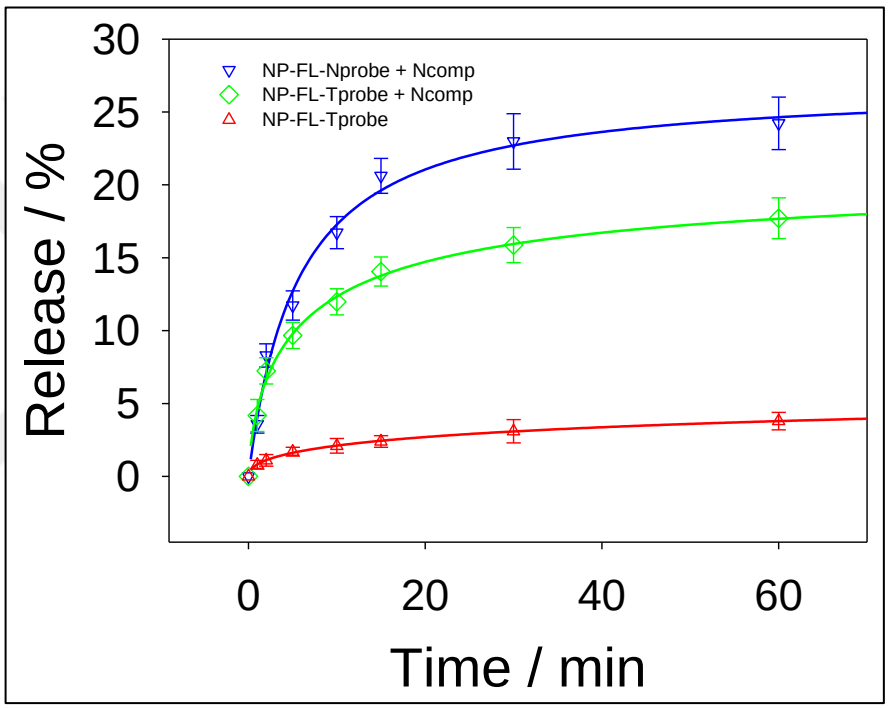

Figure 4.10. Evaluation of FL-NP-Tprobe or FL-NP-Nprobe in PBS buffer with synthetic target sequences.

The particles loaded with fluoroscein and capped with normal sequence oligonucleotides (Nprobe) were incubated in the buffer, to determine their stability and reporter molecule retention (red line). Addition of 1 μM of normal target sequence Ncomp oligonucleotide were monitored for fluorescent signal to evaluate the release of reporter by the specific hybridization (green for NP-FL-Tprobe and blue lines for NP-FL-Nprobe). All the measurements were carried out in triplicate; the results show average fluorescence intensity and the error bars represent standard deviation.

4.3. PCR AMPLIFICATION AND RELEASE ASSAY WITH REAL SAMPLES

To test the assay ability to determine IVS-110 mutations, real samples were collected and the assay procedure was applied on blood samples from 3 thalessemia patents and 3 normal person. First, the genomic DNA from blood samples were isolated and 58 bp fragment around mutation region were amplified by PCR using the primer sequences in Table 2.1 (Figure 4.8). Figure 4.11 shows that a gene sequence around IVS-110 mutation region was successfully obtained. Subsequently, a single strand speretaion procedure was performed for isolating only one strand sequence from the PCR product (non-biotinylated strand). This step was necessary because only single stranded target sequences were able to complement efficiently to Tprobe sequence caps, resulting in fluorescent signal.

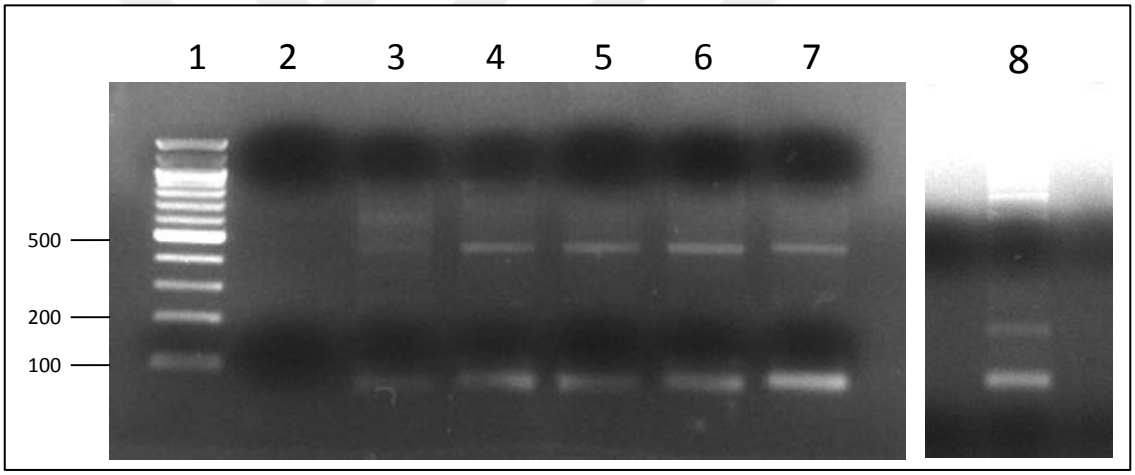

Figure 4.11. PCR results for a normal and Thalassemia patients. Lane 1: DNA ladder, Lanes 2-4: Mutated sample 1-3, Lanes 5-8: Normal sample 1-3.

The single stranded PCR products from blood samples were mixed with 0.1 mg of NP-FL-Tprobe or NP-FL-Nprobe particles and incubated for 20 min. at room temperature. The fluorescent signals were presented in Figure 4.12. For all Thalessemia positive patients (for IVS-110 mutation), the signal with NP-FL-Tprobe were higher than NP-FL-Nprobe. For normal person samples, the signals for NP-FL-Nprobe were higher than NP-FL-Tprobe as expected.

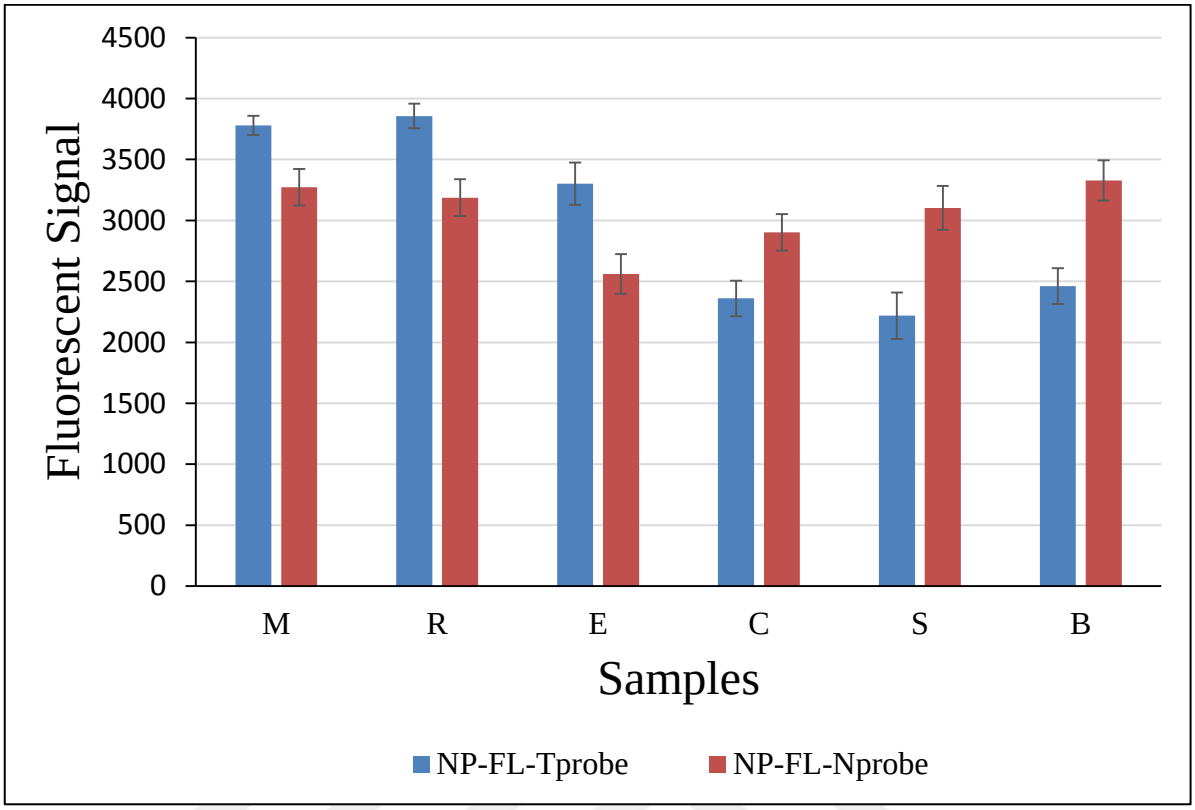

Figure 4.12. The fluorescent signals from PCR products of real samples. Samples M, R and E are Thalassemia positive patients and samples C, S and B are normal blood samples.

5. DISCUSSION

5.1. PROBE-GATED NANOPARTICLES FOR BIOSENSOR DEVELOPMENT

Molecular-gated biosensors are created by loading a porous nanopartical with a reporter molecule and then capping with a molecular mechanism, which can be triggered to open in the presence of its target [42]. Nucleic acid oligonucleotides has been used as capping element and specific trigger was sometimes hybridization with complementary oligo. For example, *Yan et. al.* designed a UV triggered reversible hybridization DNA cap [43]. Hybridization/dehybridization gates has been utilized for designing specific biosensors for mercury, miRNA, genomic mutations, etc. [44,45]. In this study, hybridization trigger was used to detect a single nucleotide mutation of Thalassemia, called IVS-110. As shown in Figure 5.1, single stranded probe oligonucleotide with perfect matching for IVS-110 mutated sequence were used to cover reporter loaded silica nanoparticles. Genomic DNA were amplified with PCR to obtain single stranded fragment of the mutated region.

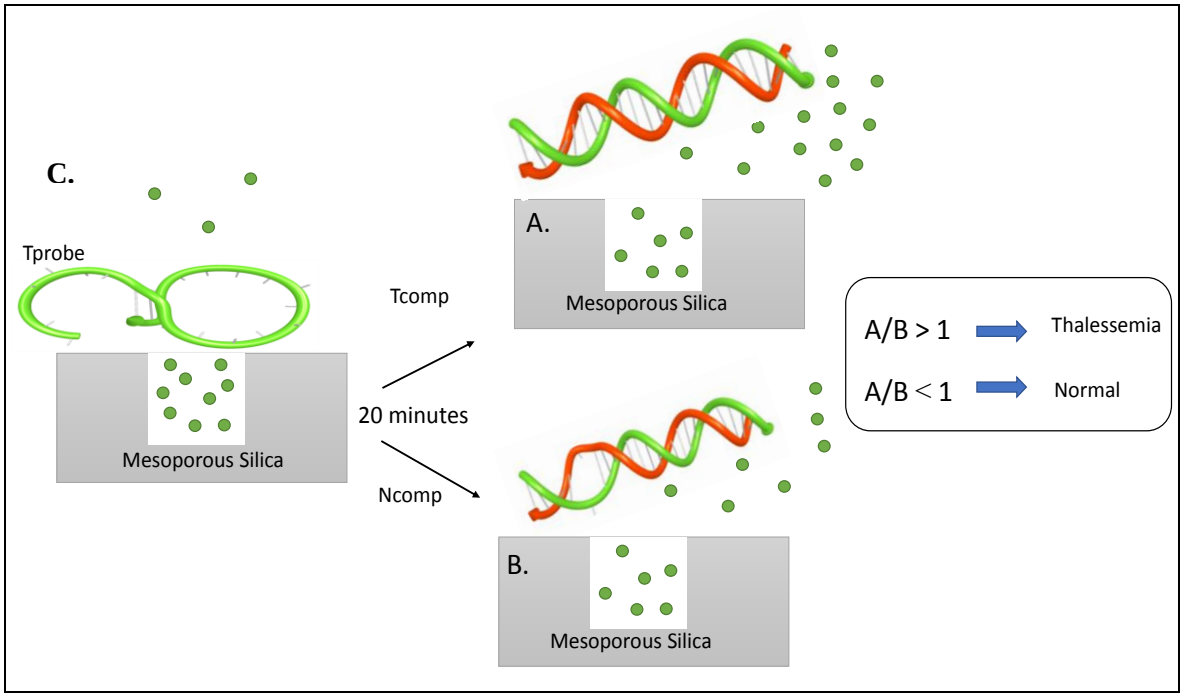

Figure 5.1. Schematic representation for fabrication of DNA probe cap, entrapping fluorescein molecules inside the pores of silica nanoparticles.

The principle of the assay system relies on triggered release of fluorophore molecules trapped inside the nanoporous voids of a nanomatrix (Figure 5.1C). The single stranded probe sequence will assume a 3D conformation based on intramolecular hybridization.

5.2. CHARACTERIZATION OF NANOPARTICLES

The MCM-41 type material were characterized as amorphous spherical particles by SEM analysis. SEM analysis generates a variety of images from electron beam signals on the surface of particles. SEM images might reveal information about external texture, chemical composition, structure and orientation of materials. SEM analysis in this study was used to obtain the image of dry material with minimal sample preparation. High vacuum and dry sample use are common limitations in nanoparticle analysis. Thus, complementary analysis is usually necessary to understand the samples in depth since the application in this study involved the use of aqueous solution of MCM-41 nanoparticles. A digital picture with known position and intensity was obtained in a SEM analysis [46]. Magnification factor of images was calculated by dividing scan distance in images to scan distance in samples. In fact, the image was kept in a fixed size and reduced the x and y scan currents to achieve the presented magnifications. The image brightness represented the specimen response to electron rays.

The characterization measurements showed that MCM-41 particles used in this study were amorphous spherical nanoparticle with 183 nm hydrodynamic diamater. The surface of the particle were covered with mesopores of hexagonal structure in 2.83 nm in diameter. This is in good aggreement with previoıs reports of MCM-41 nanoparticles in literature [39,47]. The characteristic properties determined in this study were listed in Table 5.1. The measurements were generally consistent with the Sigma-Aldrich supplier information [48].

Table 5.1. The properties of MCM-41 nanoparticles used in this study

Unit cell size	4.6-4.8 nm
Pore volume	0.98 cm3/g
Pore size	2.3-2.7 nm
Specific surface area	~1000 m2/g (BET)
Boiling Point	2230 °C
Melting Point	>1600 °C
Bulk density	0.34 g/mL
Density of silanol groups	between 10 and 15 % of the silicon centers are hydroxylated

5.3. AMINO FUNCTIONALIZATION

Biocompatible polymers are commonly functionalized with specific chemical groups such as thiol, amine or epoxy groups to modify their surface properties and/or to attach bioactive molecules like proteins or nucleic acids. A reliable method is usually required to characterize such group surface densities. In this study, amine fuctionalization was used to obtain a plus charged silica surface for subsequent adsorption of negatively charged DNA oligonucleotides. Aminated SiO_2-NPs were generated by APTES silanization method in order to have a dense positive charge surface. Among commonly used dyes for amino group quantification, Coomassie Brillant Blue (CBB) was selected to quantify the extent of amine grafting resulting from APTES derivatization procedure. CBB is a divalent dye. Such rapid and convenient colorimetric assays have been found to be comparable to surface atomic compositions obtained from X-ray photoelectron spectroscopy (XPS) measurements [49]. CBB was found to be one of the most appropriate dye for quantifying primary amine groups in a reliable and specific way. CBB very sensitive and provided reliable quantification over a wide range of amino group surface densities. Many dyes are commonly used to quantify primary amine groups onto solid surfaces. Among these, the

ability of Coomassie Brilliant Blue to quantify surface amino groups was used in terms of adsorbed densities onto aminated surfaces.

5.4. PROBE-GATED NANOPARTICLES

Figure 4.9. and 4.10. showed that a single base difference between mutated and normal sequences resulted in the reporter release rates from mesopores. To explain this phenomenon, Gibb's free energies of a perfect complementation and a single-mismatch complementation structures were calculated performing MFOLD complementation probability analysis by NUPACK, Nucleic Acid Package web application (Figure 5.2.) [50]. This demonstrated that there was a -4.16 kcal/mol energy decrease due to IVS-110 mutation (A<G). This difference indicates that lower binding affinity (less free energy) translates to slower opening of the pores and thus less fluorescent signals in case of mismatch. In another word, a probe sequence blocking pores can be more efficiently removed if there is perfect complementation.

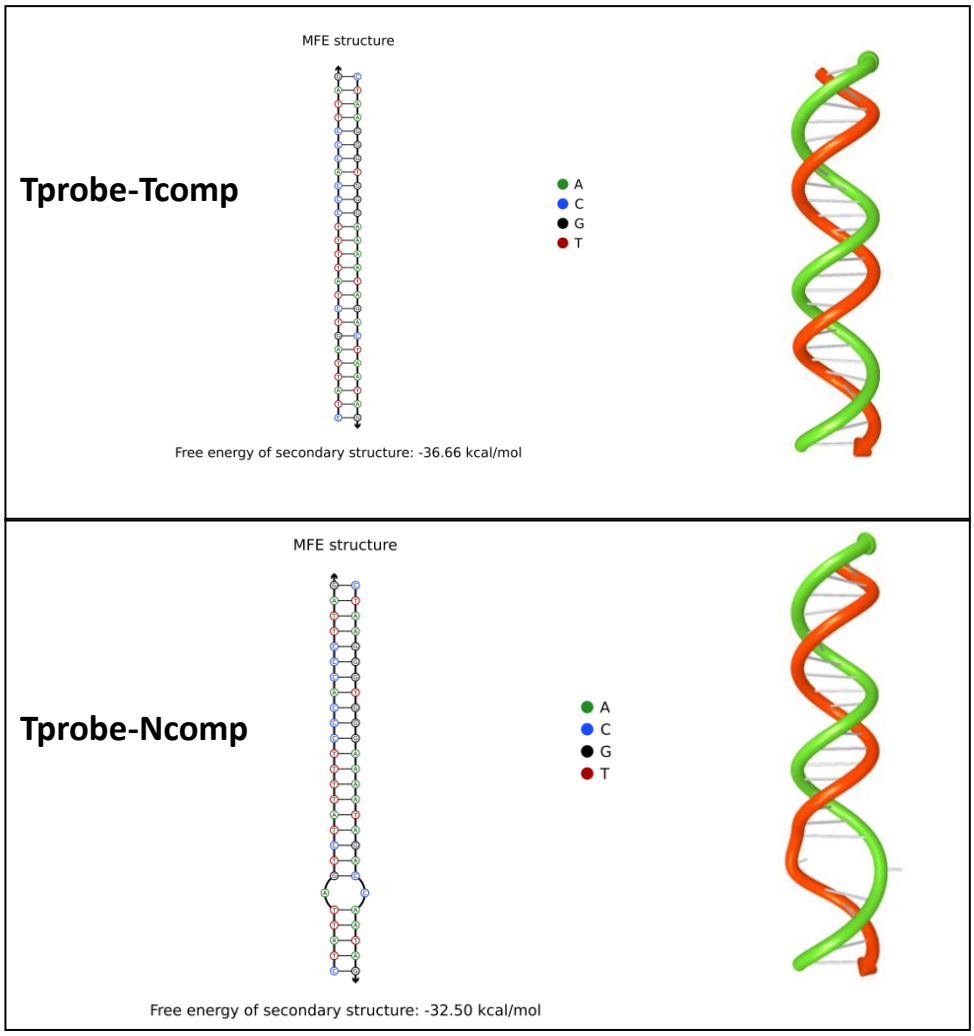

Figure 5.2. MFOLD complementation probabability analysis by NUPACK.

In Figure 5.2. assuming 1 µM concentration of each strand, probable secondary structures and their Gibb's free energy was calculated. Colored drawings at the right are 3-D depictions based on the probable structure.

5.5. ASSAY DEVELOPMENT

As shown in Figure 4.9, 20 min can be used as the assay time, which produce a distinctive signal compared to control experiments (Blue and red lines). This time period was determined as the earliest time which can produce a distinctive fluorescent signal in the experimental design as used in this study. Since the aim of this thesis was to develop a portable and rapid assay system for determination of beta-thalessemia mutation IVS-110,

this time period was considered as a reasonable assay time. As can be seeen from the results with synthetic complementary oligonucleotides, the asssay should rely on a difference between normal complementation and mutation complementation, based on a single nucleotide mismathch. Thus, a ratio of Ncomp signal and Tcomp signal were used to obtain a homogenoeus test. In this assay, a ratio value above 1 meant samples with mutated sequence or a ratio value less than 1 meant samples with normal sequence (Table 5.2.).

Table 5.2. Assay Results for Real Samples

Sample Name	**Signal NP-FL-Trobe**	**Signal NP-FL-Nrobe**	**Ratio NP-FL-Trobe/ NP-FL-Nrobe**
M	3779	3273	1.15
R	3857	3187	1.21
E	3301	2561	1.29
C	2360	2902	0.81
S	2219	3102	0.72
B	2462	3328	0.74

6. CONCLUSION

Oligonucleotide-gated mesoporous nanoparticles-based analysis is a new platform for mutation detection that has the advantages of sensitivity, rapidity, accuracy, and convenience. In this study, we used hybridization trigger to detect a single nucleotide mutation of β-Thalassemia, called IVS-110 which was used as model mutation sequence. Samples from IVS-110 mutated patients and normal individuals resulted in significant differences when the assay procedure were applied. This results demonstrate that a single nucleotide difference in the probe-target comlementation produced a detectable signal difference between mutated and normal samples.

7. FUTURE PERSPECTIVES

The genosensor design as developed in this study can be extended to assays for multiple mutations to cover all beta thalessemmia. Moreover, the principles developed in this study can be used to develop assays for many other genetic diseases. Thus, conveniently fast and affordable test formats could be created for better solutions in diagnosis of genetic diseases, whether the patient would show the associated medical conditions in her life time or she is just a carrier.

REFERENCES

1. G. Honig. Hemoglobin disorders. In: R. E. Behrman, R. Kliegman, A. M. Arvin, W. E. Nelson, editors, *Nelson textbook of pediatrics,* pages:1398-400. Philadelphia, PA: Elsevier/Saunders, United States, 1996.

2. D. J. Weatherall. Phenotype-Genotype Relationships in Monogenic Disease: Lessons from the Thalassaemias. *Nature Reviews Genetics*. 2:245-55, 2001.

3. T. H. J. Huisman. The Structure and Function of Normal and Abnormal Hemoglobins. *Bailiere's Clinical Haematology*, 6:1-30, 1993.

4. R. L. NAGEL. Disorder of Hemoglobin Function and Stability. In: R. I. Handin, S. E. Lux and T. P. Stossel, editors. *Blood: Principles and Practice of Hematology*, pages 1597-1654. Lippincott Williams and Wilkins, Philadelpphia, 2003.

5. "Hemoglobin", http://www.thealevelbiologist.co.uk/haemoglobin, [retrieved 10 November 2016].

6. G. R. Honig, and J. G. Adams. *Human Hemoglobin Genetics*, Springer-Verlag New York, Inc., New York, 1986.

7. "Heme Group" http://biomodel.uah.es/en/model3/hemoglob.htm, [retrieved 10 November 2016].

8. L. R. Manning, J. E. Russell, J. C. Padovan, B. T. Chait, A. Popowicz, R. S. Manning and J. M. Manning. Human Embryonic, Fetal, and Adult Hemoglobins Have Different Subunit Interface Strengths. Correlation with Lifespan in the Red Cell. *Protein Science : A Publication of the Protein Society*, 16:1641–58, 2007.

9. H. Fathallah and F. G. Atweh. DNA Hypomethylation Therapy for Hemoglobin Disorders: Molecular Mechanisms and Clinical Applications. *Blood Reviews*., 20:227-234, 2006.

10. V. G. Sankaran and D. G. Nathan. Reversing the Hemoglobin Switch. *The New England Journal of Medicine*, 363:2258-60, 2010.

11. D. Weatherall and A. Provan. Red cells I: Inherited Anaemias. *The Lancet*, 355:1169–1175, 2000.

12. D. N. Greene, C. P Vaugn, B. O. Crews and A. M. Agarwal. Advances in Detection of Hemoglobinopathies. *Clinica Chimica Acta*, 439:50–57, 2014.

13. M. H. Steinberg and J. G. Adams. Thalassemic Hemoglobinopathies. *The American Journal of Pathology, 113*:396–409, 1983.

14. M. L. Turgeon. *Clinical hematology: Theory and procedures, Third edition*, Lippincott Williams and Wilkins, Philadelphia, PA, 1999.

15. D. R. Higgs. Gene Regulation in Hematopoiesis: New Lessons from Thalassemia. *Hematology. American Society of Hematology. Education Program*. p:1-13, 2004.

16. D. R. Higgs, W. G. Wood, A. P. Jarman, M. A. Vickers, A. O. Wilkie, J. Lamb, P. Vyas and J. P. Bennet. The Alpha-Thalassemias. *Annals New York Academy Sciences*, 612:15-2, 1990.

17. C.L. Harteveld, D. R. Higgs. α-Thalassemia. *Orphanet Journal Rare Diseases,* 28:5-13, 2010.

18. C. K., Lin, M. L Yang, M. L., Jiang, C. C Chie, H. H. Lin and H.W. Peng. Comparison of Two Screening Methods, Modified Hb H Preparation and the Osmotic Fragility Test, for Alpha-Thalassemic Traits on the Basis of Gene Mapping. *Journal of Clinical Laboratory. Analysis,* 5:392-395, 1991.

19. J. M. Gonzalez-Redondo, T. A. Stoming, A. Kutlar, F. Kutlar, K. D. Lanclos, E. F. Howard, Y. J. Fei, M. Aksoy, C. Altay and A. Gurgey. A C → T substitution at nt −101 in a Conserved DNA Sequence of the Promoter Region of the β-globin Gene is Associated with “Silent” β-Thalassemia. *Blood,* 73:1705–1711, 1989.

20. V. Viprakasit. Alpha Thalassemia Syndromes: From Clinical and Molecular Diagnosis to Bedside Management. *European Hematology Association, Hematology Education Program*, 7:329–338, 2013.

21. M. J. Cunningham. Update on Thalassemia: Clinical Care and Complications. *Hematology/Oncology Clinics of North America*, 24:215-27, 2010.

22. S.L. Thein. β-Thalassemia. *Bailliere's Clinical Haematology*, 6:151-175, 1993.

23. V. Smolkin, R. Halevy, C. Levin, M. Mines, W. Sakran, K. Ilia and A. Koren. Renal Function in Children with Beta-Thalassemia Major and Thalassemia Intermedia. *Pediatric Nephrology*, 23:1847-51, 2008.

24. S. Kalman, A. A. Atay, O. Sakallıoğlu, T. Özgürtaş, F. Gök, I. Kurt, O. Kürekçi. Renal Tubular Fuction in Children with Beta-Thalassemia Minor. *Nephrology,* 10:427-9, 2005.

25. L. O'Connor and B. Glynn. Recent Advances in the Development of Nucleic Acid Diagnostics. *Expert Review of Medical Devices*, 7:529-534, 2010.

26. S. E. Antonarakis, P. G. Waber, S.D. Kittur, A. S. Patel, Jr H. H Kazazian, M. A. Mellis, R. B. Counts, G. Stamatoyannopoulos, E. W. Bowie and D. N. Fass. Hemophilia A Detection of Molecular Defects and of Carriers by DNA Analysis. *New England Journal of Medicine*, 313:842-848, 1985.

27. U. Landegren, R. Kaiser, C. T. Caskey and L. Hood. DNA Diagnostics--Molecular Techniques and Automation. *Science*, 242:229-237, 1988.

28. M. B. Wabuyele, H. Farquar, W. Stryjewski, R. P. Hammer, S. A. Soper, Y.-W.Cheng and F. Barany. Approaching Real-Time Molecular Diagnostics: Single-Pair Fluorescence Resonance Energy Transfer (spFRET) Detection for the Analysis of Low Abundant Point Mutations in K-ras Oncogenes. *Journal of the American Chemical Society*, 125:6937-6945, 2003.

29. D. J. Cutler, M. E. Zwick, M. M. Carrasquillo, C. T. Yohn, K. P. Tobin, C. Kashuk, D. J. Mathews, N. A. Shah, E. E. Eichler and J. A. Warrington. High-Throughput Variation Detection and Genotyping Using Microarrays. *Genome Research*, 11:1913-1925, 2001.

30. S. Dong, E. Wang, L. Hsie, Y. Cao, X. Chen and T. R. Gingeras. Flexible Use of High-Density Oligonucleotide Arrays for Single-Nucleotide Polymorphism Discovery and Validation. *Genome Research*, 11:1418-1424, 2001.

31. J. G. Hacia, J. B. Fan, O. Ryder, L. Jin, K. Edgemon, G. Ghandour, R. A. Mayer, B. Sun, L. Hsie and C. M. Robbins. Determination of Ancestral Alleles for Human Single-Nucleotide Polymorphisms Using High-Density Oligonucleotide Arrays. *Nature Genetics*, 22:164-167, 1999.

32. A. J. Schafer and J. R. Hawkins. DNA Variation and the Future of Human Genetics. *Nature Biotechnology*, 16:33-39, 1998.

33. T. LaFramboise. Single Nucleotide Polymorphism Arrays: A Decade of Biological, Computational and Technological Advances. *Nucleic Acids Research*, 37:4181–4193, 2009.

34. R. J. Watson. The Hereditary Anemias. *Bulletin of the New York Academy of Medicine*, 30:106, 1954.

35. N. Akar, A. Cavdar, E. Dessi, A. Loi, M. Pirastu and A. Cao. Beta Thalassemia Mutations in the Turkish Population. *Journal of medical genetics*, 24:378, 1987.

36. E.Ö. Atalay, H. Koyuncu, B. Turgut, A. Atalay, S. Yildiz, A. Bahadir and A. Kösele. High Incidence of Hb D-Los Angeles [β121 (GH4) Glu→ Gln] in Denizli Province, Aegean Region of Turkey. *Hemoglobin*, 29:307-310, 2005.

37. R. C. Hardison, D.H. Chui, C. Riemer, B. Giardine, H. Lehväslaiho, H. Wajcman and Miller W. Databases of Human Hemoglobin Variants and Other Resources at the Globin Gene Server. *Hemoglobin*, 25:183-193, 2001.

38. G. O. Tadmouri and A. N. Basak. β-Thalassemia in Turkey: A Review of the Clinical, Epidemiological, Molecular, and Evolutionary Aspects. *Hemoglobin*, 25:227-239, 2001.

39. V. C. Ozalp, and T. Schafer. Aptamer-Based Switchable Nanovalves for Stimuli-Responsive Drug Delivery. *Chemistry-A European Journal*, 17:9893-9896, 2011.

40. A. M. Collins. Common Analytical Techniques for Nanoscale Materials. In: A. M. Collins editor, *Nanotechnology cookbook*, pages: 32-33. Elsevier Science Publishers Ltd, London, 2012.

41. J. Li, X. Miao, Y. Hao, J. Zhao, X. Sun and L. Wang, *Journal of Colloid and Interface Science*, 318:309-314, 2008.

42. L. Pascual, I. Baroja, E. Aznar, F. Sancenon, M. D. Marcos, J. R. Murguia, P. Amoros, K. Rurack and R. Martinez-Manez, *Chemical Communications*, 51:1414-1416, 2015.

43. D. Y. Tam and P. K. Lo Multifunctional DNA Nanomaterials for Biomedical Applications. *Journal of Nanomaterials*, 2015:1-21, 2015.

44. F. Sancenón, L. Pascual, M. Oroval, E. Aznar and R. Martínez-Máñez. Gated Silica Mesoporous Materials in Sensing Applications. *Chemistry Open*, 4:418-437, 2015.

45. Y. H. Wang, L. Jiang, L. Chu, W. Liu, S. Wu, Y. H. Wu, X. X. He and K. M. Wang. Electrochemical Detection of Glutathione by Using Thymine-Rich DNA-Gated Switch Functionalized Mesoporous Silica Nanoparticles. *Biosensors and Bioelectronics*, 87:459-465, 2017.

46. R. F. Egerton. The Scanning Electron Microscope. In: R. F. Egerton editor, *Physical Principles of Electron Microscopy*, pages 125-153. Springer-Verlag New York, Inc., New York, 2005.

47. H. Chen and Y. Wang. Preparation of MCM-41 with high thermal stability and complementary textural porosity. *Ceramics International.* 28:541–547, 2002.

48. Sigma-Aldrich, 643645. "Silica mesostructured, MCM-41 type (Hexogonal)", http://www.sigmaaldrich.com [retrieved 11 November 2016].

49. S. Noel, B. Liberelle, L. Robitaille and G. D. Crescenzo. Quantification Of Primary Amine Groups Available For Subsequent Biofunctionalization Of Polymer Surfaces. *Bioconjugate Chemistry*, 22:1690–1699, 2011.

50. J. N. Zadeh, C. D. Steenberg, J. S. Bois, B. R. Wolfe, M. B. Pierce. NUPACK: Analysis and Design Of Nucleic Acid Systems. *Journal of Computational Chemistry*, 32:170-173, 2011